A Maximum Likelihood Tracker for Multistatic Sonars

Orlando D.
DAEIMI
Università degli Studi di Cassino
Via G. Di Biasio 43, 03043 Cassino, Italy
danilo.orlando@unisalento.it

Ehlers F.
NATO Undersea Research Centre (NURC)
Viale S. Bartolomeo 400
19126 La Spezia, Italy
ehlers@nurc.nato.int

Ricci G.
Dip. di Ing. dell'Innovazione
Università del Salento
Via Monteroni, 73100 Lecce, Italy
giuseppe.ricci@unisalento.it

Abstract – ***In this paper, we propose a TBD like tracker designed to work in a multistatic sonar environment where measurements collected by different sensors are sent to a fusion center. A preliminary performance assessment, carried out by Monte Carlo simulation, is also provided. Finally, we test the newly proposed algorithm with a benchmark dataset provided by METRON in the context of collaborative international multi-laboratory research that is ongoing in the ISIF*** **Multi-Static Tracking Working Group*****. The preliminary analysis shows that the proposed algorithm has acceptable performance also when the probability of detection per sensor is low (in the order of 0.3) and measurement errors are significant.***

Keywords: Data association, likelihood ratio, estimation, multi-sensor, tracking.

1 Introduction

Traditional tracking algorithms are designed assuming that the sensor provides a set of discrete measurements at each scan (or ping). In an activated surveillance system such measurements could be obtained by thresholding the output of a matched filter fed by a baseband version of collected data. Then, the tracking algorithm links measurements across time and estimates the parameters of interest. The threshold value must be low enough to guarantee a sufficiently high probability of target detection. However, a low threshold gives rise to a high rate of false alarms. It follows that to avoid false tracks it is necessary to effectively solve the data association problem [1]. A reliable means of validating the track estimate as a target-originated one is also required.

An alternative approach, developed to track low signal-to-noise ratio (SNR) targets, consists of track-before-detect (TBD) techniques. TBD-based procedures jointly process several consecutive pings and, relying on target kinematics or, simply, exploiting the physically admissible target transitions, declare the presence of a target and, eventually, its track [2, 3, 4, 5, 6]. A TBD algorithm is typically fed by unthresholded data or thresholded data with significantly lower threshold than the ones used by conventional trackers. Moreover, a TBD scheme ensuring the constant false alarm rate (CFAR) property with respect to the unknown statistics of the disturbance controls the overall false track acceptance rate (CFTAR property).

In this work, we focus our attention on a sensor network which provides a set of time difference of arrival and bearing information over one or more targets on M consecutive pings. More precisely, we consider an underwater surveillance system consisting of multiple acoustic sound sources and multiple receivers. This setup is called *multistatic sonar* and leads to an increased detection performance and accuracy in target state estimation. The main idea behind the TBD paradigm is then applied to the overall dataset in order to process all measurements and obtain a track estimate assuming the presence of one maneuvering target only in the surveillance region.

Notice that in the considered system sensors make hard decisions and transmit these results (also including side informations) to the fusion center for track estimate. In other words, we consider a parallel fusion network employing centralized fusion architecture. Moreover, we assume that the target motion is deterministic and maximize the likelihood function of the measurements (depending on the target position at each ping) by resorting to a Viterbi-like procedure [5, 6, 7]. A preliminary performance assessment is also provided and

it is carried out by Monte Carlo simulation.

Finally, we test the newly proposed algorithm with a benchmark dataset provided by METRON [8] in the context of collaborative international multi-laboratory research that is ongoing in the ISIF *Multi-Static Tracking Working Group*.

The paper is organized as follows. Section 2 is devoted to the description of the surveillance sonar system while Section 3 contains the derivation of the proposed tracker. In Section 4 some illustrative examples are given. Finally, Section 5 contains some concluding remarks and potential directions for future work.

2 System Description

The considered scenario involves

- N_s sources that alternately illuminate the surveillance region of size A with a ping occurring every T_p seconds; the N_s-source ping schedule is

$$j = [(m-1) \mod N_s] + 1, \tag{1}$$

  where j is the index of the transmitting source at the mth ping and $[a \mod b]$, $a, b \in \mathbb{N}$, is the remainder of the division a/b.

- N_r synchronous receivers.

Source and receiver positions are known. Each receiver provides a set of measurements (or contacts), namely

$$\begin{aligned} &\boldsymbol{Z}_{i,m} = \{\boldsymbol{z}_{i,1,m}, \ldots, \boldsymbol{z}_{i,N_{i,m},m}\}, \\ &i = 1, \ldots, N_r, \ m = 1, \ldots, M, \end{aligned} \tag{2}$$

where M is the total number of illuminations and $N_{i,m}$ is the number of measurements collected by the ith receiver at the mth ping. As to the $\boldsymbol{z}_{i,m}$'s, they are two-dimensional vectors defined as

$$\boldsymbol{z}_{i,m} = \begin{bmatrix} d_{i,m} \\ \theta_{i,m} \end{bmatrix}, \tag{3}$$

where $\theta_{i,m}$ is the bearing measured clockwise from the receiver north and $d_{i,m}$ denotes the time difference of arrival (TDOA) between the direct blast and the contact.

In the following we assume that when a measurement has originated from the target, the corresponding errors are normally distributed, more precisely

$$e_{d_{i,m}} \sim \mathcal{N}_1(0, \sigma_d^2), \tag{4}$$

$$e_{\theta_{i,m}} \sim \mathcal{N}_1(0, \sigma_\theta^2), \tag{5}$$

where $\sigma_d > 0$ and $\sigma_\theta > 0$ are the standard deviations of the TDOA error and of the bearing error, respectively. Both σ_d and σ_θ are known. On the other hand, when the contacts are due to the noise, we assume that they

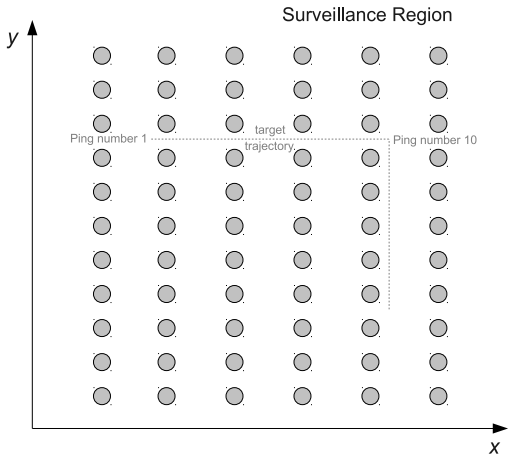

Figure 1: Grid of points covering the surveillance reagion.

are uniformly distributed in the measurement space, namely

$$d_{i,m} \sim \mathcal{U}(d_{i,m}^{\min}, d_{i,m}^{\max}), \tag{6}$$

$$\theta_{i,m} \sim \mathcal{U}(\theta_{i,m}^{\min}, \theta_{i,m}^{\max}). \tag{7}$$

where

- $d_{i,m}^{\min}$ and $d_{i,m}^{\max}$ is the minimum and maximum TDOA for the ith receiver at the mth ping, respectively;

- $\theta_{i,m}^{\min}$ and $\theta_{i,m}^{\max}$ is the minimum and maximum bearing for the ith receiver at the mth ping, respectively.

3 Maximum Likelihood Track Estimator

In this section we derive a procedure to estimate the target trajectory by using the overall dataset denoted by

$$\boldsymbol{Z} = \{\boldsymbol{Z}_{1,1}, \ldots, \boldsymbol{Z}_{1,M}, \ldots, \boldsymbol{Z}_{N_r,1}, \ldots, \boldsymbol{Z}_{N_r,M}\}. \tag{8}$$

To this end, we define a grid of points

$$G = \{(x_i, y_j)\}_{\substack{i=1,\ldots,N_x \\ j=1,\ldots,N_y}} \tag{9}$$

which covers the entire surveillance region as shown in Figure 1 and assume that the target is moving through the points of G. Moreover, let

$$\boldsymbol{x}_m = \begin{bmatrix} x_m \\ y_m \end{bmatrix} \in G \tag{10}$$

the position of the target at the mth ping and $j_{i,m}$, $i = 1, \ldots, N_r$, $m = 1, \ldots, M$, an integer indexing target originated contacts for the ith receiver at the mth ping.

Assuming that, given the sequence of target positions over M pings

$$\boldsymbol{X} = [\boldsymbol{x}_1 \cdots \boldsymbol{x}_M], \tag{11}$$

the measurements are each other independent, it is not difficult to show that the probability density function of $\boldsymbol{Z}$ can be written as follows

$$f_1(\boldsymbol{Z}; \boldsymbol{X}, \boldsymbol{J}) = \prod_{m=1}^{M} \prod_{i=1}^{N_r} \left\{ \frac{(1 - P_{i,m})}{(U_{i,m})^{N_{i,m}}} + P_{i,m} \frac{f(\boldsymbol{z}_{i,j_{i,m},m}; \boldsymbol{x}_m)}{(U_{i,m})^{N_{i,m}-1}} \right\}, \tag{12}$$

where

$$\boldsymbol{J} = [\boldsymbol{j}_1 \cdots \boldsymbol{j}_M], \text{ with } \boldsymbol{j}_m = \begin{bmatrix} j_{1,m} \\ \vdots \\ j_{N_r,m} \end{bmatrix}, \tag{13}$$

$$U_{i,m} = \left(d_{i,m}^{\max} - d_{i,m}^{\min}\right) \left(\theta_{i,m}^{\max} - \theta_{i,m}^{\min}\right), \tag{14}$$

$P_{i,m}$ is the probability of detection of the ith receiver at the mth ping[1], and

$$f(\boldsymbol{z}_{i,j_{i,m},m}; \boldsymbol{x}_m) = \frac{1}{2\pi\sigma_d^2\sigma_\theta^2} \times \exp\left\{ -\frac{1}{2} \boldsymbol{y}_{i,j_{i,m},m}^T \boldsymbol{R}^{-1} \boldsymbol{y}_{i,j_{i,m},m} \right\} \tag{15}$$

with, in turn,

$$\boldsymbol{y}_{i,j_{i,m},m} = \boldsymbol{z}_{i,j_{i,m},m} - \boldsymbol{z}_{i,j}(\boldsymbol{x}_m) \tag{16}$$

and

$$\boldsymbol{R} = \begin{bmatrix} \sigma_d^2 & 0 \\ 0 & \sigma_\theta^2 \end{bmatrix}. \tag{17}$$

In (16), $\boldsymbol{z}_{i,j}(\boldsymbol{x}_m)$ is a vector valued function with vector argument that converts coordinates (x_m, y_m) into TDOA and bearing with respect to the ith receiver and the jth source (given by equation (1)).

Dividing equation (12) by the pdf of $\boldsymbol{Z}$ under the noise-only hypothesis, given by

$$f_0(\boldsymbol{Z}) = \prod_{m=1}^{M} \prod_{i=1}^{N_r} \frac{1}{U_{i,m}^{N_{i,m}}}, \tag{18}$$

we obtain the likelihood ratio

$$\Lambda(\boldsymbol{Z}; \boldsymbol{X}, \boldsymbol{J}) = \prod_{m=1}^{M} \prod_{i=1}^{N_r} \{(1 - P_{i,m}) + P_{i,m} f(\boldsymbol{z}_{i,j_{i,m},m}; \boldsymbol{x}_m) U_{i,m}\}, \tag{19}$$

which, by taking the logarithm, becomes

$$\Lambda(\boldsymbol{Z}; \boldsymbol{X}, \boldsymbol{J}) = \sum_{m=1}^{M} \sum_{i=1}^{N_r} \log \{(1 - P_{i,m}) + P_{i,m} f(\boldsymbol{z}_{i,j_{i,m},m}; \boldsymbol{x}_m) U_{i,m}\}. \tag{20}$$

[1]We assume that $P_{i,m}, \forall i, m$, is known.

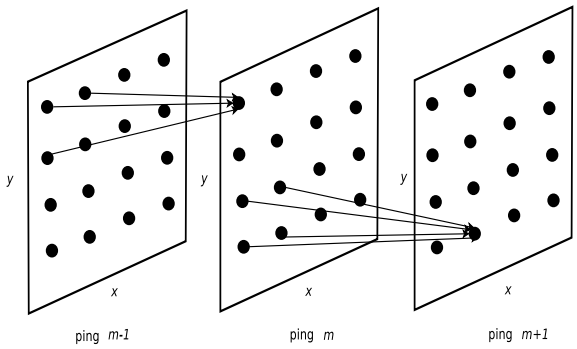

Figure 2: The expanded trellis whose states are the points of G.

Observe that the likelihood ratio (20) is a function of the target positions $\boldsymbol{X}$ and of the target originated measurement index $\boldsymbol{J}$, which are unknown and, consequently, have to be estimated. To this end, we resort to the maximum likelihood approach and maximize (20) with respect to $\boldsymbol{X}$ and $\boldsymbol{J}$.

The optimization with respect to $\boldsymbol{j}_m$, $m = 1, \ldots, M$, is straightforward and solves the data association problem; in fact, for each receiver it is possible to select the measurement index $\widehat{j}_{i,m}$ which minimizes the following distance

$$\boldsymbol{y}_{i,j_{i,m},m}^T \boldsymbol{R}^{-1} \boldsymbol{y}_{i,j_{i,m},m}, \quad i = 1, \ldots, N_r, \quad m = 1, \ldots, M. \tag{21}$$

It follows that (20) can be recast as

$$\Lambda(\boldsymbol{Z}; \boldsymbol{X}, \widehat{\boldsymbol{J}}) = \sum_{m=1}^{M} \sum_{i=1}^{N_r} \log \{(1 - P_{i,m}) + P_{i,m} f(\boldsymbol{z}_{i,\widehat{j}_{i,m},m}; \boldsymbol{x}_m) U_{i,m}\}, \tag{22}$$

where

$$\widehat{\boldsymbol{J}} = \left\{ \widehat{j}_{i,m} \right\}_{\substack{i = 1, \ldots, N_r \\ m = 1, \ldots, M}} \tag{23}$$

Finally, we estimate the sequence of target positions

$$\widehat{\boldsymbol{X}} = \arg\max_{\boldsymbol{X}} \Lambda(\boldsymbol{Z}; \boldsymbol{X}, \widehat{\boldsymbol{J}}) \tag{24}$$

resorting to a Viterbi-like procedure to find the best path metrics in an expanded trellis diagram of depth M whose states are the points of G (see Figure 2). Such a procedure relies on the assumption that target velocity vector is somewhat constrained (see also Figure 3).

An important remark is now in order. The grid G is obtained by spatially sampling the surveillance region and, given the time interval between consecutive pings, the minimum inter-point spacing specifies the minimum (nonzero) target velocity between two consecutive pings. It follows that if we restrict the search

algorithm to the set of physically admissible trajectories by limiting the maximum number of point transitions in the expanded trellis diagram, we are implicitly defining a discrete and finite set of possible target velocities. This comes in handy to incorporate, when it is available, the Doppler information of the target in the proposed algorithm.

4 Performance Assessment

In this section we provide some illustrative examples to show the effectiveness of the newly proposed algorithm. To this end, we consider $N_r = 12$ hydrophones (Rx) placed in the positions listed in Table 1 and $N_s = 4$ sources positioned as shown in Table 2. Moreover, we assume

$$P_{i,m} = P_d, \ \forall i, m. \tag{25}$$

The surveillance region is a 16740×16740 m^2 square with the upper left corner at $(37500, 34500)$ m and it is covered by a grid of 31×31 points 540 m spaced apart. Such a separation corresponds to a nominal target velocity of 6 knots. The total number of processed ping is $M = 20$ and the time interval between consecutive pings is $T_p = 180$ seconds. As to the synthetic target, we assume that it moves within the surveillance area with a constant velocity of about 6 knots and that after 10 pings its direction of motion changes as shown in Figure 1. See Table 3 for more details on the target motion. The standard deviations of target originated measurements are set as follows

$$\sigma_d = 0.4 \text{ sec} \quad \text{and} \quad \sigma_\theta = 8 \text{ degrees}, \tag{26}$$

while for each couple source-receiver the false contacts are distributed uniformly in the bistatic ellipse that contains the surveillance region. Finally, the number of false contacts, namely those not originated from the target, obeys to the Poisson distribution with parameter $\lambda = P_{fa} N_{\text{cell}}$, where P_{fa} is the probability of false alarm in any cell and N_{cell} is the total number of cells. All simulation results assume $P_{fa} = 0.01$ and $\lambda = 9.6$.

Table 1: Hydrophone coordinates.

Rx number	X (meters)	Y (meters)
1	26752,91	8219,99
2	26752,91	26740
3	26752,91	45259,99
4	45285,83	8219,99
5	45285,83	45259,99
6	63818,75	8219,99
7	63818,75	26740
8	63818,75	45259,99
9	36033,99	17479,99
10	36033,99	36000
11	54581,52	17479,99
12	54581,52	36000

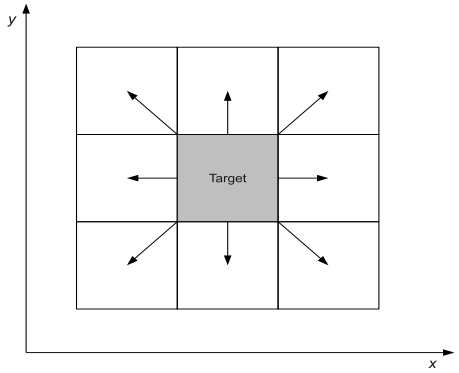

Figure 3: Possible motion directions of the target.

Table 2: Projector coordinates.

Sr number	X (meters)	Y (meters)
1	17486.46	54520
2	54581,52	17480
3	54581,52	54520
4	17486.46	17480

Table 3: Target Motion.

Ping number	X (meters)	Y (meters)
1	40200	29640
2	40740	29640
3	41280	29640
4	41820	29640
5	42360	29640
6	42900	29640
7	43440	29640
8	43980	29640
9	44520	29640
10	45060	29640
11	45060	29100
12	45060	28560
13	45060	28020
14	45060	27480
15	45060	26940
16	45060	26400
17	45060	25860
18	45060	25320
19	45060	24780
20	45060	24240

In Figures 4-8 we show the estimated tracks from 4 independent trials. Each figure refers to different values of P_d and reports the actual trajectory of the target (ground truth). Observe that for low values of P_d ($P_d = 0.2, 0.3$) the proposed algorithm is still capable of providing an estimate of the target positions, even

though the estimation error is significant. On the other hand, for greater values of P_d the estimated target locations closely follow the ground truth. Such results are confirmed by Figures 9 and 10, where we plot the root mean square (RMS) values based on 300 independent trials versus the P_d. Finally, in Figures 11 and 12 we illustrate the results obtained by applying the proposed algorithm to the first MSTWG METRON dataset.

5 Conclusions

In this paper, we have proposed a TBD like tracker designed to work in a multistatic sonar environment where measurements collected by different sensors are sent to a fusion center. A preliminary performance assessment, carried out on simulated scenarios, shows that the proposed algorithm has acceptable performance also when the probability of detection per sensor is low (in the order of 0.3) and measurement errors are significant. Ongoing research activity is aimed at incorporating doppler and SNR measurements in the tracker.

References

[1] Y. Bar-Shalom and T. E. Fortmann, *Tracking and Data Association*, Academic Press, 1988.

[2] J. D. R. Kramer and J. W. S. Reid, "Track-before-detect processing for an airborne type radar," *In Proc. of IEEE 1990 International Radar Conference*, Arlington, VA, USA, May 1990, pp. 422-427.

[3] W. R. Wallace, "The use of track-before-detect in pulse-doppler radar," *In Proc. of IEEE 2002 International Radar Conference*, Edinburgh, UK, October 2002, pp. 315-319.

[4] S. Buzzi, M. Lops, and L. Venturino, "Track-before-detect procedures for early detection of moving target from airborne radars," *IEEE Transactions on Aerospace and Electronic Systems*, Vol. 41, No. 3, pp. 937-954, July 2005.

[5] D. Orlando, L. Venturino, M. Lops, and G. Ricci, "Track-Before-Detect Strategies for STAP Radars," *IEEE Transactions on Signal Processing*, Vol. 58, No. 2, pp. 933-938, February 2010.

[6] D. Orlando, F. Ehlers, and G. Ricci, "Track-before-detect Algorithms for Bistatic Sonars," *In proc. of the 2nd International Workshop on Cognitive Information Processing*, Elba Island, Italy, June 2010.

[7] G. D. J. Forney, "The Viterbi algorithm," *Proc. IEEE*, Vol. 29, No. 3, pp. 268-277, March 1973.

[8] K. Orlov, Description of the "MetronSimulation" dataset for the MSTWG, *METRON Technical Memorandum*, June 2009.

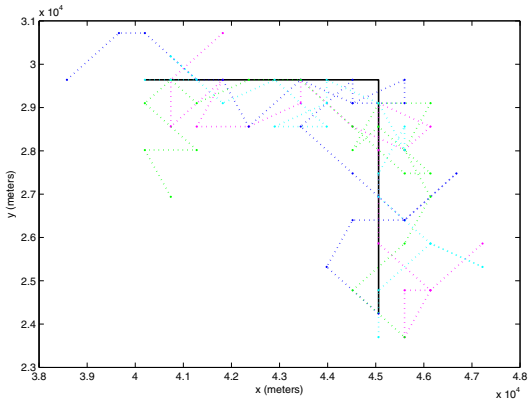

Figure 4: Estimated tracks from 4 independent trials (dotted line with dot marker) and ground truth (solid line) assuming $P_d = 0.2$.

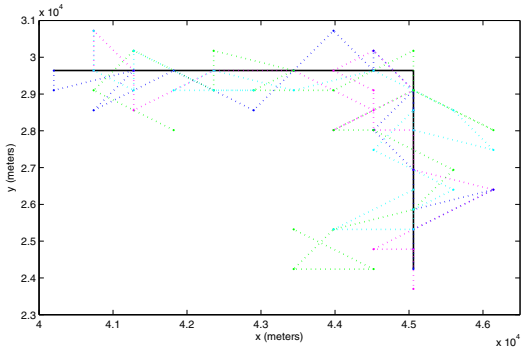

Figure 5: Estimated tracks from 4 independent trials (dotted line with dot marker) and ground truth (solid line) assuming $P_d = 0.3$.

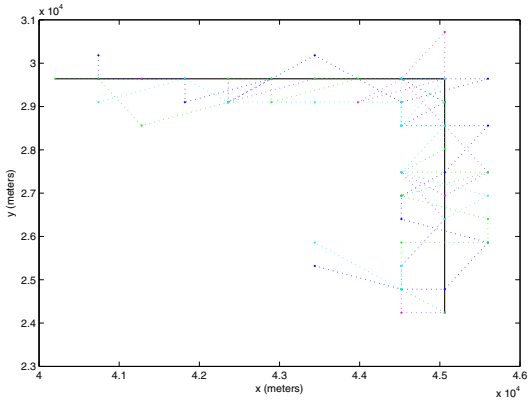

Figure 6: Estimated tracks from 4 independent trials (dotted line with dot marker) and ground truth (solid line) assuming $P_d = 0.5$.

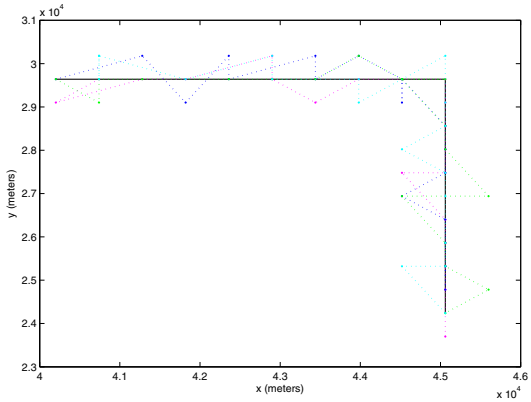

Figure 7: Estimated tracks from 4 independent trials (dotted line with dot marker) and ground truth (solid line) assuming $P_d = 0.8$.

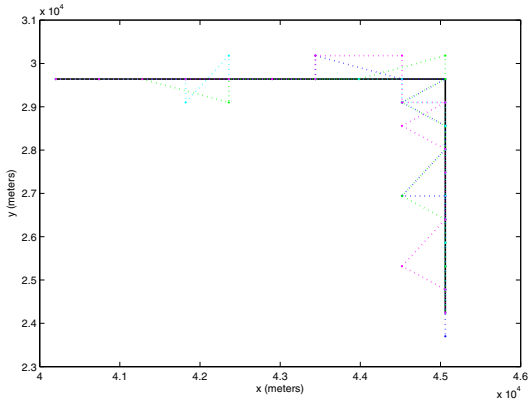

Figure 8: Estimated tracks from 4 independent trials (dotted line with dot marker) and ground truth (solid line) assuming $P_d = 1$.

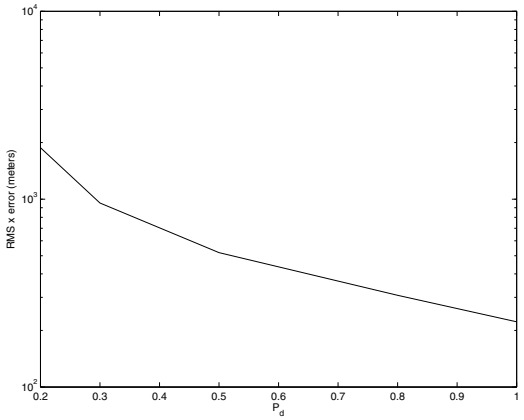

Figure 9: RMS error in x versus P_d.

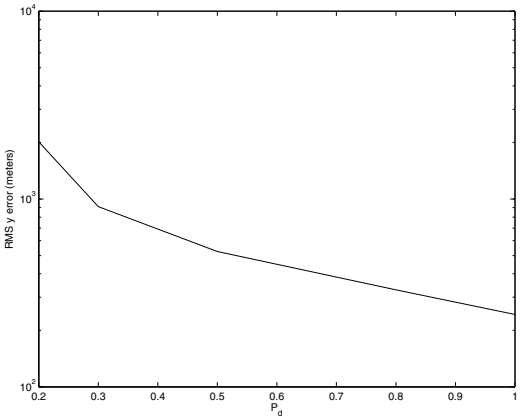

Figure 10: RMS error in y versus P_d.

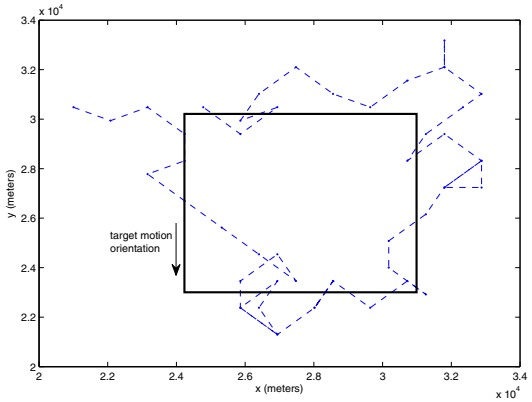

Figure 11: Estimated track (dashed line with dot marker) and ground truth (solid line) for the third target of the first MSTWG METRON dataset.

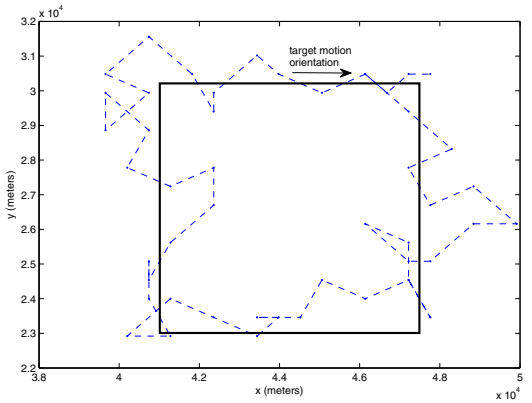

Figure 12: Estimated track (dashed line with dot marker) and ground truth (solid line) for the fourth target of the first MSTWG METRON dataset.